Deep inelastic neutron scattering off D_2 and H_2 and momentum distributions of nuclei in diatomic molecules

C. Andreani and A. Filabozzi
Dipartimento di Fisica, Università di Roma Tor Vergata, Via della Ricerca Scientifica 1, Roma, Italy

E. Pace
Dipartimento di Fisica e Istituto Nazionale di Fisica Nucleare Sezione Tor Vergata, Università di Roma Tor Vergata, Via della Ricerca Scientifica 1, Roma, Italy

(Received 5 July 1994; revised manuscript received 24 October 1994)

A quantum-mechanical calculation for the description of neutron scattering at very high momentum transfer off both homonuclear and heteronuclear diatomic molecules at $T=0$ K in terms of the nuclear momentum distribution, $n(k)$, of the nuclei in these molecules is proposed. The results of this calculation compare well with neutron-scattering measurements on liquid D_2 at $T=20$ K in the momentum transfer range $55<q<80$ Å^{-1} and with previous measurements on solid H_2 at $T=4$ K and liquid H_2 at $T=20$ K at high momentum transfer ($q\sim100$ Å^{-1}), showing that high-energy neutrons can be a sensitive probe to investigate the momentum distribution of the nuclei in these molecules.

I. INTRODUCTION

In recent years the inelastic neutron scattering at energy transfer up to 150 eV, has grown in importance as a research tool. Indeed it is now possible to perform inelastic-scattering experiments at large energy transfer, and hence high-momentum transfer, using the epithermal flux of neutrons available from spallation sources.[1] In this scattering regime, known as deep-inelastic neutron scattering (DINS), the experimental determination of the atomic momentum distributions in condensed matter is based on the assumption that the impulse approximation (IA) is valid.[2] In this respect it is possible to find in DINS conceptual elements and calculational approaches common to other techniques, namely, Compton scattering of x rays and γ rays used for the determination of electron distributions in solids,[3] and quasielastic electron scattering off nucleons in nuclei, used for the determination of nucleon momentum distributions.[4]

Recently DINS experiments have been performed on various atomic and molecular fluids and solids composed of atoms of relatively low mass, namely, H_2 (Refs. 5 and 6) and ^{4}He (Refs. 7 and 8) in condensed phases. In the measurements on diatomic molecules, performed on liquid and solid H_2, the kinetic energy for the parahydrogen *molecule* in the solid at 10 K and in the liquid at 17 K has been assessed[5] and the kinetic energy in solid parahydrogen at 4.7 K and various molar volumes has been also derived.[6] In both measurements the center-of-mass translational energy per molecule was determined from the width of the recoil peaks and a variety of peaks corresponding to internal molecular transitions from ground ($J=0$) to excited rotational ($J=1,3,5,7$) and vibrational states were observed. Indeed, due to the moderate range in energy transverse available, $\hbar\omega<1500$ meV, the recoiling particle was the whole H_2 molecule. In this context it is of great interest the scattering off H_2 and D_2 at higher energy and momentum transfer since, as it will be shown in the following, in this latter case the recoil occurs from a single *nucleus* within the molecule at an energy transfer of $\hbar\omega_R=\hbar^2q^2/2M$, being M the mass of the struck nucleus and q the momentum transfer in the scattering process. Hence in this scattering regime DINS is probing the momentum distributions of nuclei within these molecules and can provide useful information on the wave function for the motion of the nuclei in the ground state of these systems.[9]

In this paper a theoretical calculation at $T=0$ K for the description of neutron scattering at high-momentum transfer in terms of the nuclear momentum distribution, $n(k)$, of the deuterium in D_2 and proton in H_2 is proposed and is extended to include the case of heteronuclear diatomic molecules. The quantum-mechanical calculation relies on the assumption that the final state for the struck *nucleus* is a plane wave and makes no use of free parameters. The result of this calculation provides an asymptotic scaling function, $F(y)$,[10] which at high energy (3000–6500 meV) and momentum transfer ($55<q<80$ Å^{-1}) compares quite well with the experimental data on liquid D_2 at $T=20$ K obtained in a DINS experiment, performed at ISIS on the eVS spectrometer. Furthermore our calculation is able to reproduce the experimental scaling function of solid and liquid H_2 (at $T=4$ and 20 K, respectively) at high-momentum transfer ($q\sim100$ Å^{-1}) presented in a previous paper,[9] where a model calculation, including some free parameters, was used to describe the data.

The results of the present paper show the reliability of our approach in describing the inelastic neutron scattering at high-momentum transfer from solids and liquids composed of diatomic molecules and confirm that DINS is the proper experimental technique to investigate the single-particle dynamics in condensed phases, although it is envisaged that the experimental resolution may play a

crucial role and smooth out relevant features of the scaling function in a substantial way.

II. THEORETICAL CALCULATION

Let us consider the response function at high energy and momentum transfer for the neutron scattering off homonuclear diatomic molecules, e.g., D_2, at very low temperature (say $T \leq 20$ K) in the medium:

$$S(q,\omega)=\sum_f \left|\left\langle \Phi_f \left| \sum_{j=1}^{2} e^{i\mathbf{q}\cdot\mathbf{r}_j} \right| \Phi_i \right\rangle\right|^2 \delta(\hbar\omega+E_i-E_f) . \quad (1)$$

In Eq. (1), Φ_i and Φ_f are the initial- and final-state wave functions for the orbital motion of the two nuclei, E_i and E_f the initial and final energies of the system, and $\mathbf{r}_1,\mathbf{r}_2$ the coordinates of the nuclei. At high-momentum transfer the interference terms in Eq. (1) can be neglected. Since each of the nuclei gives the same response, the response for a single nucleus is

$$\bar{S}(q,\omega)=\frac{S(q,\omega)}{2} =\sum_f |\langle \Phi_f | e^{i\mathbf{q}\cdot\mathbf{r}_1} | \Phi_i \rangle|^2 \delta(\hbar\omega+E_i-E_f) . \quad (2)$$

The orbital initial-state wave function of the nuclei can be written as follows:

$$\Phi_i=\varphi_i(\mathbf{r})\Psi_i^m(\mathbf{R}) , \quad (3)$$

where $\varphi_i(\mathbf{r})$ describes the relative motion of the two nuclei and $\Psi_i^m(\mathbf{R})$ describes the motion of the center of mass in the medium. The coordinate $\mathbf{R}=(\mathbf{r}_1+\mathbf{r}_2)/2$ is the coordinate of the center of mass of the nuclei, which essentially coincides with the center of mass of the molecule, and $\mathbf{r}=\mathbf{r}_1-\mathbf{r}_2$ is the relative coordinate. At $T \leq 20$ K the equilibrium concentration for orthodeuterium ($J=0$) is $c_0 \geq 96.5\%$ and for paradeuterium ($J=1$) $c_1 \leq 3.5\%$.[11] Therefore in this case it is a reasonable assumption to regard the molecule in the orthostate only. In this state the relative wave function has angular momentum $J=0$ and can be cast in the following form:

$$\varphi_i(\mathbf{r})=\frac{1}{r}u_v(r)\varphi_J^{\mathrm{rot}}(\theta,\varphi) , \quad (4)$$

where $u_v(r)$ describes the vibrational motion of the nuclei and $\varphi_J^{\mathrm{rot}}(\theta,\varphi)=\varphi_0^{\mathrm{rot}}(\theta,\varphi)=1/\sqrt{4\pi}$ is the angular wave function.

At higher values of the momentum transfer, one can approximate with a plane wave the wave function of the nucleus struck by the incident neutron. Therefore the wave function of the nuclei in the final state can be expressed as follows:

$$\Phi_f(\mathbf{r})=\frac{1}{(2\pi)^{3/2}}e^{i\mathbf{k}_1'\cdot\mathbf{r}_1}\psi_{f_2}(\mathbf{r}_2) , \quad (5)$$

where $\mathbf{k}_1'$ is the final momentum of the struck nucleus and $\psi_{f_2}(\mathbf{r}_2)$ is the final state of the other nucleus with energy ε_{f_2}.

By performing the substitution $\mathbf{k}_1=\mathbf{k}_1'-\mathbf{q}$, the dynamical structure factor becomes

$$\bar{S}(q,\omega)=\int d\mathbf{k}_1 \sum_{f_2} \left| \int d\mathbf{r}_1 d\mathbf{r}_2 \frac{e^{-i\mathbf{k}_1\cdot\mathbf{r}_1}}{(2\pi)^{3/2}} \psi_{f_2}^*(\mathbf{r}_2)\Phi_i(\mathbf{r},\mathbf{R}) \right|^2 \times\delta\left[\hbar\omega+E_i-\frac{\hbar^2k_1^2}{2M}-\frac{\hbar^2q^2}{2M}-\frac{2\hbar^2\mathbf{k}_1\cdot\mathbf{q}}{2M}-\varepsilon_{f_2}\right] . \quad (6)$$

If the scaling variable y

$$y=\frac{M}{\hbar^2 q}\left[\hbar\omega-\frac{\hbar^2q^2}{2M}\right] \quad (7)$$

and the scaling function

$$F(q,y)=\frac{\hbar^2 q}{M}\bar{S}(q,\omega) \quad (8)$$

are introduced, then the terms independent of q in the energy conservation δ function become negligible at high q, and the asymptotic scaling function in the limit $q\rightarrow\infty$ is

$$F(y)=\int d\mathbf{k}_1 \sum_{f_2} \left| \int d\mathbf{r}_1 d\mathbf{r}_2 \frac{e^{-i\mathbf{k}_1\cdot\mathbf{r}_1}}{(2\pi)^{3/2}} \psi_{f_2}^*(\mathbf{r}_2)\Phi_i(\mathbf{r},\mathbf{R}) \right|^2 \times\delta(y-\mathbf{k}_1\cdot\hat{\mathbf{q}}) , \quad (9)$$

where $\hat{\mathbf{q}}=\mathbf{q}/|\mathbf{q}|$. Using the closure relation to eliminate $\sum_{f_2}$ one obtains

$$F(y)=\int d\mathbf{k}_1 n_1(\mathbf{k}_1)\delta(y-\mathbf{k}_1\cdot\hat{\mathbf{q}}) =2\pi\int_{|y|}^{\infty} k_1 n_1(k_1) dk_1 . \quad (10)$$

In Eq. (10) the momentum distribution, $n_1(\mathbf{k}_1)$, for the deuteron nucleus in the liquid D_2 has been introduced:

$$n_1(\mathbf{k}_1)=\int d\mathbf{r}_2 \left| \int d\mathbf{r}_1 \frac{e^{-i\mathbf{k}_1\cdot\mathbf{r}_1}}{(2\pi)^{3/2}} \Phi_i(\mathbf{r},\mathbf{R}) \right|^2 =8\int d\mathbf{k}\, n^m(2\mathbf{k}_1-2\mathbf{k})\cdot n(\mathbf{k}) , \quad (11)$$

and in the last step of Eq. (10) the independence of $n_1(\mathbf{k}_1)$ of the direction of $\mathbf{k}_1$ has been assumed. In Eq. (11),

$$n(\mathbf{k})=\left| \int d\mathbf{r} \frac{e^{-i\mathbf{k}\cdot\mathbf{r}}}{(2\pi)^{3/2}} \varphi_i(\mathbf{r}) \right|^2 \quad (12)$$

is the square of the Fourier transform of the relative wave function in the initial state, i.e., the momentum distribution for the relative motion of the nuclei in D_2. And

$$n^m(\mathbf{p})=\left| \int d\mathbf{R} \frac{e^{-i\mathbf{p}\cdot\mathbf{R}}}{(2\pi)^{3/2}} \Psi_i^m(\mathbf{R}) \right|^2 \quad (13)$$

is the momentum distribution of the center-of-mass motion of the D_2 molecule in the medium. The momentum distributions $n(\mathbf{k})$ and $n^m(\mathbf{p})$ are normalized according to $\int n(\mathbf{k})d\mathbf{k}=1$ and $\int n^m(\mathbf{p})d\mathbf{p}=1$, provided that the wave functions $\varphi_i(\mathbf{r})$ and $\Psi_i^m(\mathbf{R})$ are properly normalized.

The asymptotic scaling function can be expressed in a different form by placing the right-hand side of Eq. (11) in Eq. (10) and changing the order of integration over $\mathbf{k}_1$ and $\mathbf{k}$ and the integration variable from $\mathbf{k}_1$ to $\mathbf{p}'=\mathbf{k}_1-\mathbf{k}$:

$$\begin{aligned} F(y) &= 8\int d\mathbf{k}\int d\mathbf{k}_1 n(\mathbf{k}) n^m(2\mathbf{k}_1-2\mathbf{k})\delta(y-\mathbf{k}_1\cdot\hat{\mathbf{q}}) \\ &= 8\int dy'\int d\mathbf{k}\int d\mathbf{p}' n(\mathbf{k}) n^m(2\mathbf{p}')\delta(y'-\mathbf{p}'\cdot\hat{\mathbf{q}}) \\ &\quad \times\delta(y-y'-\mathbf{k}\cdot\hat{\mathbf{q}}) \\ &= 2\int_{-\infty}^{\infty} dy' F^m(2y') F_i(y-y') \ . \end{aligned} \tag{14}$$

In Eq. (14),

$$F^m(y)=\int_{|y|}^{\infty} d\mathbf{p} n^m(\mathbf{p})\delta(y-\mathbf{p}\cdot\hat{\mathbf{q}}) \tag{15}$$

and

$$F_i(y)=\int_{|y|}^{\infty} d\mathbf{k} n(\mathbf{k})\delta(y-\mathbf{k}\cdot\hat{\mathbf{q}}) \tag{16}$$

are the distributions of the minimum longitudinal momentum y for the motion of the D_2 molecule in the medium and for the relative motion of the nuclei in D_2, respectively. In Eq. (14), it appears that the asymptotic scaling function $F(y)$ is the convolution of two longitudinal momentum distributions to be considered separately, one for the vibrational motion and one for the translational motion. If the momentum distributions $n(\mathbf{k})$ and $n^m(\mathbf{p})$ are independent of the directions of $\mathbf{k}$ and $\mathbf{p}$, Eqs. (15) and (16) become $F^m(y)=2\pi\int_{|y|}^{\infty} dp\, p\, n^m(p)$ and $F_i(y)=2\pi\int_{|y|}^{\infty} dk\, k\, n(k)$, respectively. This is the case for liquid orthodeuterium. Indeed in this case the initial relative wave function has angular momentum $J=0$ and then the momentum distribution $n(\mathbf{k})$ is clearly independent of the direction of $\mathbf{k}$. An another expression for $F(y)$, based only on a model calculation, has been recently proposed in Ref. 9.

In the case of neutron scattering at high momentum transfer off diatomic molecules whose nuclei have different masses M_1 and M_2, two different peaks, centered at $\hbar\omega_1=\hbar^2q^2/2M_1$ and at $\hbar\omega_2=\hbar^2q^2/2M_2$, should be observed, corresponding to the scattering off nuclei 1 and 2, respectively. The definition of the scaling variable, $y^{(j)}$, for the scattering off nucleus jth ($j=1,2$) is obtained from Eq. (7) by replacing the mass M by the mass M_j. The scaling function for the scattering off nucleus jth is defined by $F^{(j)}(y^{(j)})=S(q,\omega)(\hbar^2q/M_j)$ and can be obtained from the right-hand side of Eq. (14) be replacing both the factor 2 which multiplies the integral and the factor 2 in the argument of F^m by the factor $(M_1+M_2)/M_j$.

In order to compute $n(\mathbf{k})$ for D_2 we can try to approximate the radial wave function $u_v(r)$ corresponding to the ground state ($v=0$) with a harmonic-oscillator wave function. Within this approximation the momentum distribution $n(\mathbf{k})$ becomes

$$\begin{aligned} n(\mathbf{k}) &= \frac{4\pi}{(2\pi)^3}\frac{1}{k^2}\left[\frac{\mu\omega_0}{\hbar\pi}\right]^{1/2} \\ &\quad \times\left|\int_0^{\infty} dr \sin(kr) e^{-(\mu\omega_0/2\hbar)(r-r_0)^2}\right|^2 , \end{aligned} \tag{17}$$

where $\mu=M/2$ is the reduced mass, r_0 the equilibrium distance of the nuclei in D_2, and ω_0 the oscillator frequency. The momentum distribution $n(\mathbf{k})$, computed using for the equilibrium distance and the oscillator frequency the known values,[12] that is $r_0=0.74$ Å and $\omega_0=365$ meV, is reported in Fig. 1. The corresponding longitudinal distribution $F_i(y)$ calculated using Eqs. (16) and (17) is plotted in Fig. 2 by a solid line.

The momentum distribution for the translational motion has been described as a Gaussian function according to

$$n^m(p)=\frac{1}{(2\pi\sigma_T^2)^{3/2}} e^{-p^2/2\sigma_T^2} \tag{18}$$

and then the distribution $F^m(y)$ becomes

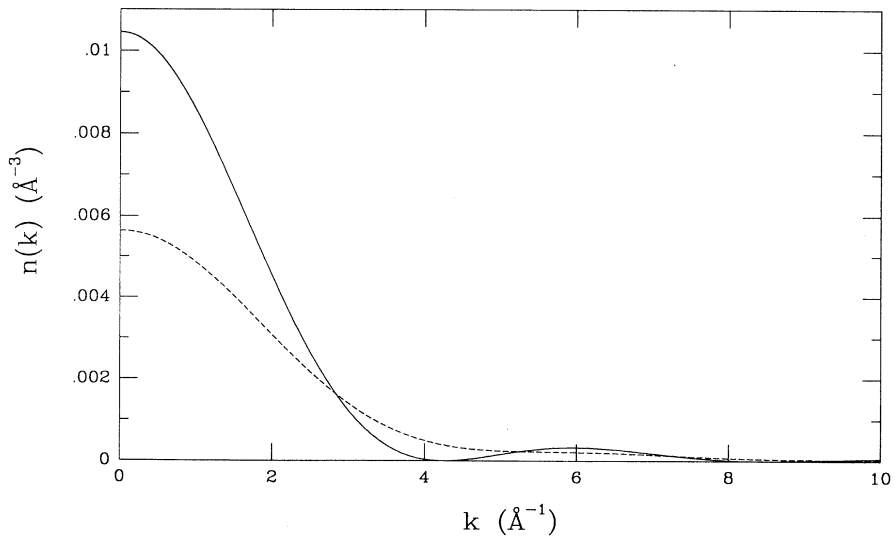

FIG. 1. Theoretical momentum distribution, $n(k)$ (solid line), corresponding to the relative vibrational motion of the deuteron nuclei in D_2 [Eqs. (12) and (17)] and total momentum distribution of the deuteron nucleus in the liquid D_2, $n_1(k_1)$ (dashed line), obtained by convolution with the translational momentum distribution [Eq. (11)].

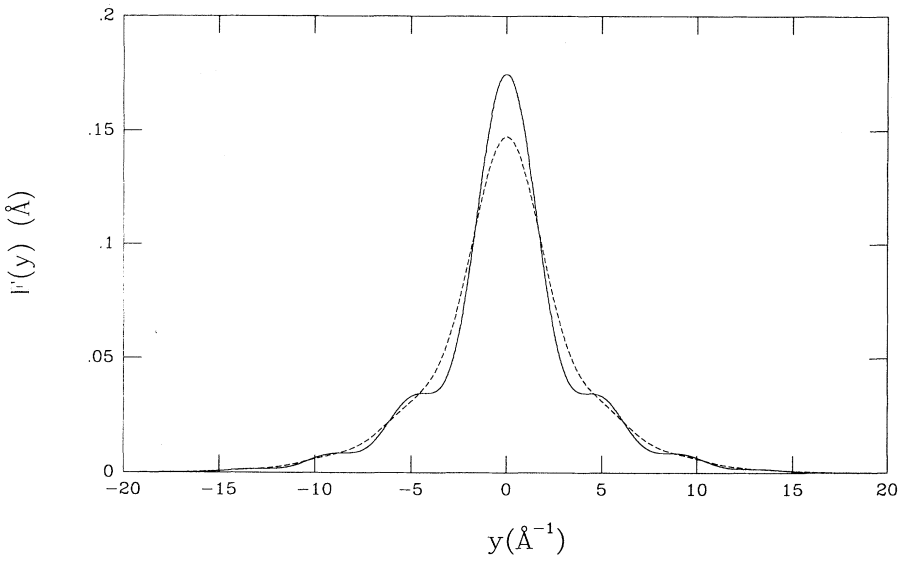

FIG. 2. Theoretical longitudinal momentum distribution, $F_i(y)$ (solid line), corresponding to the relative motion of the nuclei in D_2 [Eq. (16)] and asymptotic scaling function of the deuteron nucleus in liquid D_2, $F(y)$ (dashed line) obtained by a convolution of $F_i(y)$ with the translational longitudinal momentum distribution [Eq. (14)].

$$F^m(y)=\frac{1}{\sqrt{2\pi\sigma_T^2}}e^{-y^2/2\sigma_T^2}\ , \tag{19}$$

where σ_T, the variance of these Gaussians, represents the root-mean-square value of the longitudinal component of the molecular translational momentum in $\hbar$ units. The quantity σ_T is related to the translational kinetic energy of each molecule via

$$\sigma_T=\sqrt{2M_{D_2}\langle E_k\rangle_{D_2}/3\hbar^2}\ , \tag{20}$$

M_{D_2} being the mass of the D_2 molecule and $\langle E_k\rangle_{D_2}$ the mean kinetic energy per molecule, i.e., $\langle E_k\rangle_{D_2}=\frac{3}{2}KT^*$ (T^* being the "effective temperature" of the system[13]). In order to evaluate the kinetic energy at the temperature of our experiment quantum effects have to be taken into account. A reasonable picture of the temperature dependence of $\langle E_k\rangle_{D_2}$, inclusive of the quantum effects, can be obtained from an Einstein model, once the zero-point kinetic energy for liquid D_2 is known.[8] The latter was estimated from previous measurements on solid and liquid H_2, by scaling $\langle E_k\rangle_{H_2}$, at the same molar volume of D_2 (see below) in the assumption of a harmonic potential acting on each molecule. From Eq. (20) one yields $\sigma_T=2.2$ Å^{-1} and then $n^m(\mathbf{p})$ [Eq. (18)] and $F_m(y)$ [Eq. (19)] can be calculated. The corresponding momentum distribution $n_1(\mathbf{k}_1)$ [Eq. (11)] and the asymptotic scaling function $F(y)$ [Eqs. (10) and (14)] are reported, as dashed lines, in Figs. 1 and 2, respectively. From these figures it appears that the convolution with the translational motion smooths out considerably the oscillations of $n(k)$ and $F_i(y)$.

We would like to stress that our calculation can be applied to other diatomic molecules which have angular momentum $J=0$, as, for example, H_2 at very low temperature, with only obvious changes in the values of the physical parameters.

III. THE DINS EXPERIMENT ON LIQUID D_2

DINS experiment on liquid D_2 was performed at eVS, an inverse geometry spectrometer (IGS), installed at the Spallation Neutron Source (ISIS) at Rutherford Appleton Laboratory (UK). In this spectrometer the energy of the scattered neutrons are determined by a resonance foil located on the scattering flight path. Two kinds of measurements were performed on each sample: one with the resonance foil in the beam, and one with the foil out of the beam. By performing the difference between the foil-in and foil-out spectrum one determines the inelastic-scattering pattern of the sample. An important aspect from the experimental point of view is the best resolution one can achieve in this kind of measurement, and the most critical parameter to this aim is the choice of the resonance foil. Indeed there are various contributions to the resolution in the minimum longitudinal momentum, Δy, coming from Gaussian uncertainties in time and in the primary and secondary flight path lengths, as well as from the Lorentzian uncertainty from the resonance energy of the foil. However, the latter is the more severe one and for low mass samples a gold foil is usually the recommended choice, since it provides a compromise between intensity and resolution in y space.[1,13]

The experiment was performed on liquid deuterium at 20 K (molar volume $V=23.5$ cm^3/mole). The sample container was an aluminium plane slab with an internal thickness of 1 mm. The intensities from the sample in the container and the empty container were recorded by ^{3}He gas detectors placed around the sample, covering 20 scattering angles ranging from $2\theta=36°$ to $2\theta=77°$ (see Table I). Placing a gold resonance foil in between the sample position and detectors, the scattering signal was derived by the difference technique referred above. The momentum transfer range explored in this experiment was 32–80 Å^{-1}. The principal components of the resolution function for DINS experiments in inverse geometry spectrometers on pulsed sources can been calculated

TABLE I. Parameters of the resolution function at the scattering angles of the present experiment; the variance, σ_G, of the Gaussian component of the Voigt resolution function, $R(q,y)$, and the width, σ_L, of the Lorentzian component are reported for each angle, together with the momentum transfer corresponding to the maximum of the recoil peak.

2θ (degree)	σ_G (Å^{-1})	σ_L (Å^{-1})	q (Å^{-1})
36.00	0.914	2.272	31.9
38.10	0.885	2.151	33.9
39.85	0.862	2.061	35.7
41.85	0.840	1.968	37.7
43.70	0.822	1.889	39.6
45.87	0.802	1.806	41.8
47.80	0.788	1.739	43.7
49.70	0.772	1.679	45.8
51.65	0.762	1.622	47.8
53.70	0.749	1.567	50.1
57.60	0.733	1.475	54.7
59.80	0.722	1.430	57.5
61.95	0.715	1.390	59.8
64.10	0.708	1.353	62.4
66.10	0.702	1.322	65.1
68.42	0.696	1.289	67.5
70.50	0.691	1.262	70.2
72.65	0.689	1.236	73.3
74.75	0.685	1.214	75.8
76.92	0.682	1.193	78.7

directly in atomic momentum space[13] or derived by performing a proper experimental calibration using higher atomic mass samples, i.e., vanadium, lead, etc.[14] Both approaches allow one to estimate the values for the relative contributions to the total resolution function coming from the uncertainties in energy, scattering angle and time and their general trend as a function of the energy of the resonance foil and the atomic mass. The total resolution in momentum space, $R(q,y)$, is described by a Voigt function with a Gaussian component of variance σ_G and a Lorentzian component of width σ_L.[13] For our particular experimental data set both components are listed in Table I for the different scattering angles 2θ.

Experimental data have been corrected using a standard procedure in which the data originally in time of flight are transformed in energy transfer and then container scattering is subtracted.[1] A further correction, to take into account the multiple scattering contribution, has been also performed. This contribution, using a procedure described in Ref. 15, was found to be only a few percent of the total.

The position in energy transfer of the recoil peak for the sample is plotted in Fig. 3 as a function of $\hbar^2q^2/2$, together with a least-squares-fit straight line. It is clear that the relationship $\hbar\omega_R=\hbar^2q^2/2M$ holds and from the slope of the straight line, it appears that neutrons recoil from a particle of mass $M^{\text{expt}}=2.007\pm0.006$ (a.m.u.), which we can identify with a single deuteron nucleus of mass $M=2.0135$ (a.m.u.). This, as already observed, is a direct consequence of the high energy and momentum transfers available in the present experiment. Therefore, the value M of the mass was used to construct the scaling variable y [Eq. (7)] and the corresponding experimental scaling function from the experimental response [Eq. (8)], here after named $F_R^{\text{expt}}(q,y)$. This function for each angle includes the contribution from the resolution function, $R(q,y)$, according to

$$F_R^{\text{expt}}(q,y)=\int_{-\infty}^{+\infty}F^{\text{expt}}(q,y')\cdot R(q,y-y')dy' \quad (21)$$

In Fig. 4, the $F_R^{\text{expt}}(q,y)$ functions are plotted as a function of y, for a couple of scattering angles in the low q range and four scattering angles in the highest q range. One can note the small variation of q in the y range around the recoil peak at each angle (e.g., for $-10<y<10$ Å^{-1}) and the substantial variation in q for the different scattering angles (see top abscissas in different plots of Fig. 4). In Figs. 4(a) and 4(b) some clear shift of the experimental peak positions towards $y<0$ values is visible. This feature is a consequence of the scaling violating effects present at the finite q values avail-

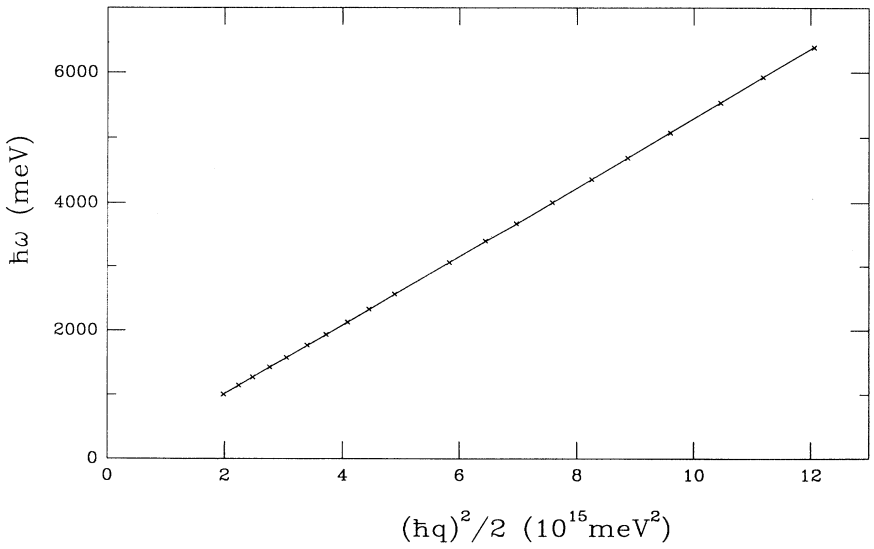

FIG. 3. Energy transfer of the recoil peak (crosses) as a function of $\hbar^2q^2/2$ for the 20 experimental scattering angles of Table I. The straight line is a least-squares fit of the data.

able in the experiments (e.g., at finite q the q independent terms in the energy conservation [see Eq. (6)] are not negligible and can produce such a shift). It is also evident that the shift of the peaks decreases by increasing the scattering angle, and becomes negligible at high momentum transfer. A final comment to Fig. 4 is that, although the overall shape of the experimental scaling function is the same, its peak intensity increases by increasing 2θ. This means, as already observed, that some q dependence is still present in the experimental scaling function

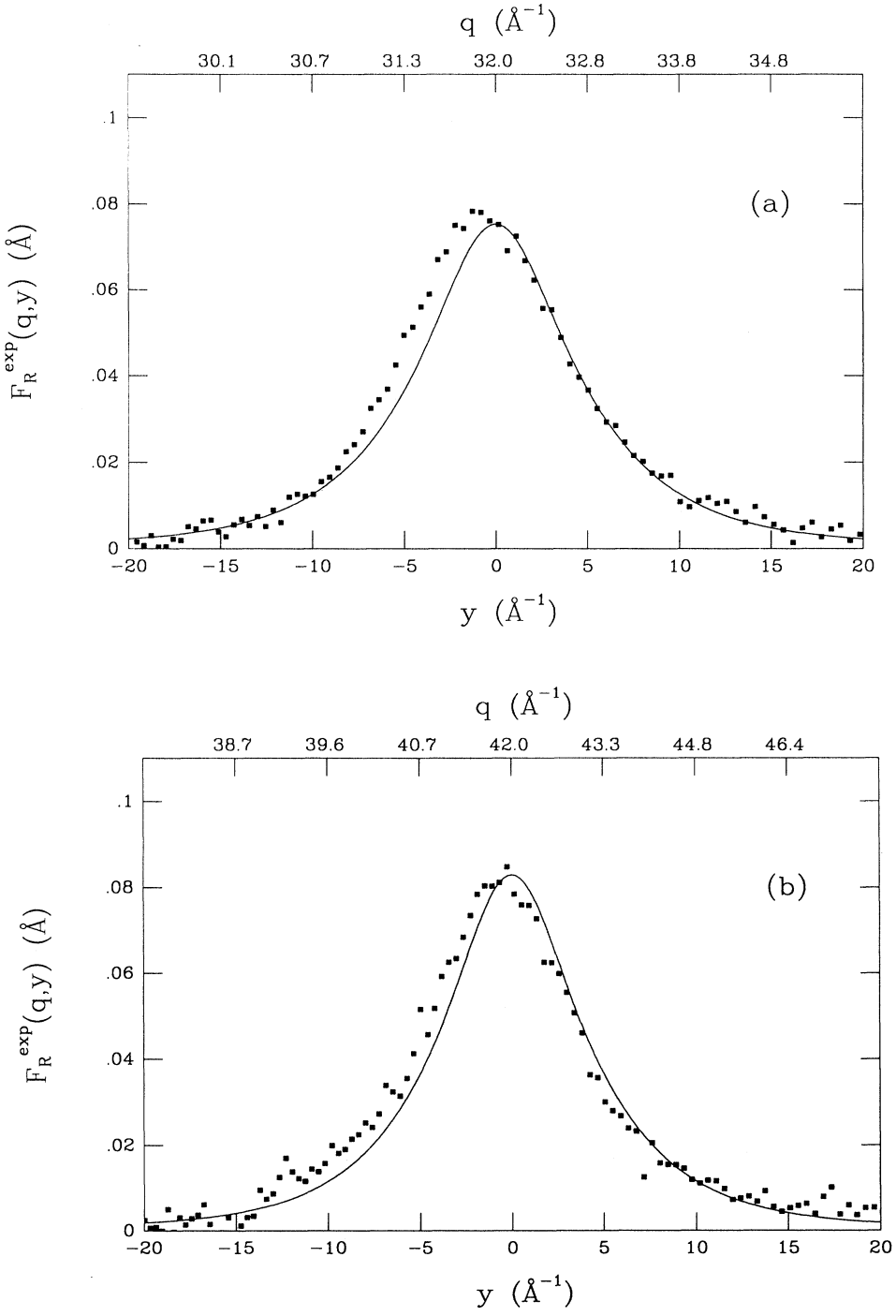

FIG. 4. Experimental scaling function, $F_R^{expt}(q,y)$ [Eq. (21)] (dots), compared with the theoretical scaling function, $F_R(q,y)$ [Eq. (22)] (solid line): (a) $2\theta=36.00°$; (b) $2\theta=45.87°$; (c) $2\theta=57.60°$; (d) $2\theta=68.42°$; (e) $2\theta=70.50°$; (f) $2\theta=74.75°$. Lower abscissa is the scaling variable, y, and top abscissa the momentum transfer, q.

$F_R^{expt}(q,y)$. Some of this q dependence is due to scaling violating effects which originate from the fact that one is dealing, strictly speaking, with a function not obtained in the asymptotic limit[16] and some to the effects of the resolution contribution, which varies with the scattering angles for this specific sample as shown in Table I.[13] A more detailed study about the approach of the experimental scaling function to its asymptotic value, $F^{expt}(y)$, and a suggested procedure for obtain the latter function, will be addressed in a paper to follow.

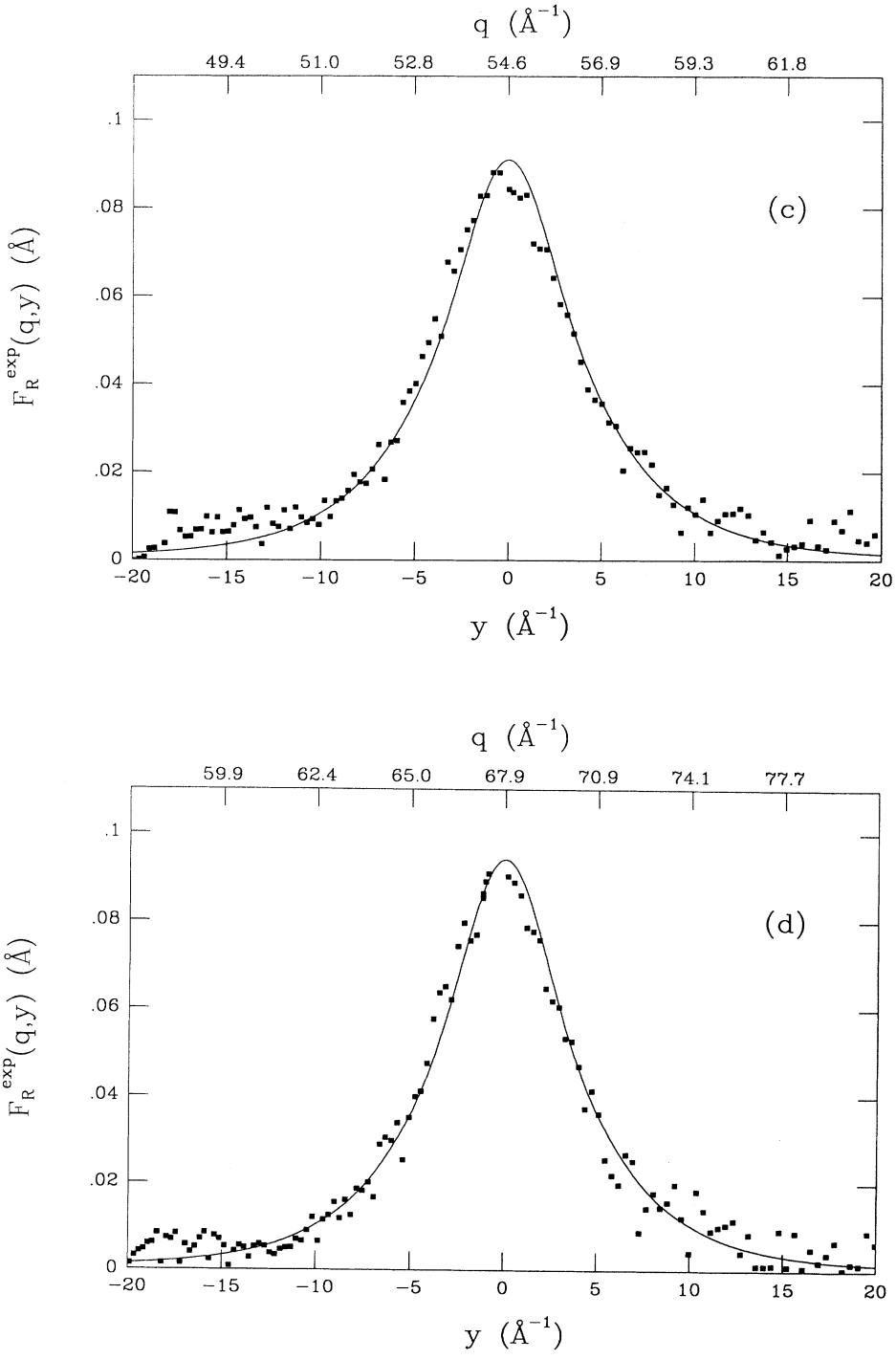

FIG. 4. (*Continued*).

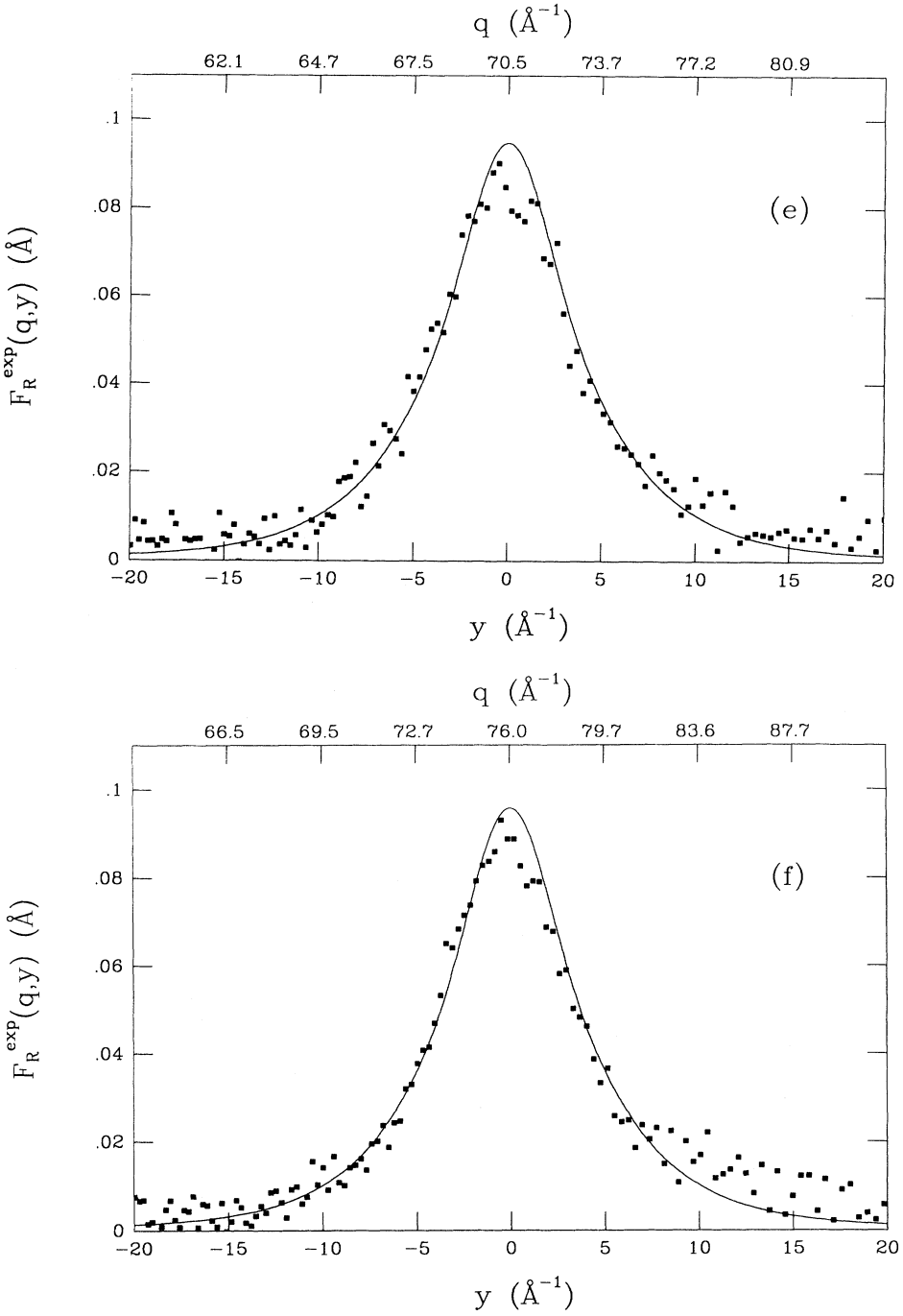

FIG. 4. (*Continued*).

IV. DISCUSSION

A comparison between theoretical calculations and the experimental data for liquid D_2 at high q values can be made by assuming that the scaling violating effects discussed in Sec. III represent a little contribution to the $F_R^{expt}(q,y)$ function. In order to take into account the variation of the experimental resolution with q we have calculated the theoretical $F_R(q,y)$ functions, that is the convolution of the asymptotic scaling function derived by our calculation, $F(y)$ [see Eqs. (10) and (14)], with the experimental resolution of each set of data. This procedure yields

$$F_R(q,y)=\int_{-\infty}^{+\infty}F(y')\cdot R(q,y-y')dy' \ . \tag{22}$$

In Fig. 4, together with the $F_R^{expt}(q,y)$ functions, the theoretical $F_R(q,y)$ functions are also plotted as solid lines, at the various scattering angles. Unfortunately the statistical accuracy of the present set of data intrinsically

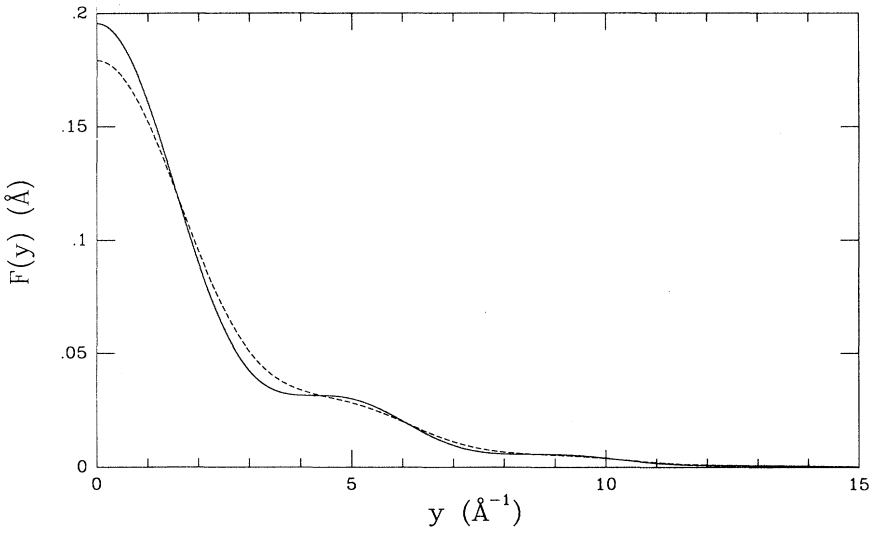

FIG. 5. Theoretical longitudinal momentum distribution, $F_i(y)$ (solid line), for H_2 [Eq. (16)] and asymptotic scaling function of the proton nucleus in H_2, $F(y)$ (dashed line) obtained by a convolution of $F_i(y)$ with the translational longitudinal momentum distribution [Eq. (14)]. Parameters used are $E_k=70$ K, $M=1$ a.m.u., $r_0=0.74$ Å, and $\sigma_T=1.4$ Å^{-1}.

limits a fully satisfactory comparison between the calculation and the experiment. From this figure one observes that the theoretical asymptotic scaling function gives for high scattering angles ($q>55$ Å^{-1}) a satisfactory agreement with experimental data, while is unable to describe the data at the lower momentum transfers, where scaling violating effects are present. From the comparison of Figs. 2 and 4, one can also note that the intensity of the calculated scaling function is greatly reduced by including the effect of the experimental resolution, even at the highest scattering angles. This is a consequence of the poor resolution available in the present experiment which smooths out considerably the waving features in $F(y)$. Indeed in the present data set $R(q,y)$, at the highest scattering angle, has a FWHM$=3.2$ Å^{-1}, whereas the asymptotic scaling function, $F(y)$, for D_2 has a FWHM~ 5.1 Å^{-1} (see Fig. 2). The latter function is itself derived from another convolution between the vibrational longitudinal distribution $F_i(y)$, Eq. (14), with the translational distribution $F^m(2y)$, whose FWHM is 2.59 Å^{-1}. Therefore any oscillatory behavior of $F_i(y)$, visible from Fig. 2 (solid line), is heavily smoothed out from a first convolution with the translational motion and a second one with the experimental resolution.

For this reason another check on the reliability of our calculation has been performed by comparing theoretical and experimental scaling functions in the case of H_2, where, due to the lower recoil mass, resolution contribution is less severe. Furthermore, in the case of H_2 the translational kinetic energy, known from previous experiments (see Refs. 6 and 7), gives $\sigma_T=1.4$ Å^{-1}, smaller than for D_2 due to the lower atomic mass.[8] In Fig. 5, the $F_i(y)$ [Eq. (16)] and $F(y)$ [Eq. (14)] functions are shown and in Fig. 6 our theoretical result, $F_R(q,y)$, is compared with $F_R^{\text{expt}}(q,y)$ function from Ref. 9 for solid H_2 at $T=4$ K and liquid H_2 at $T=20$ K in the high-momentum

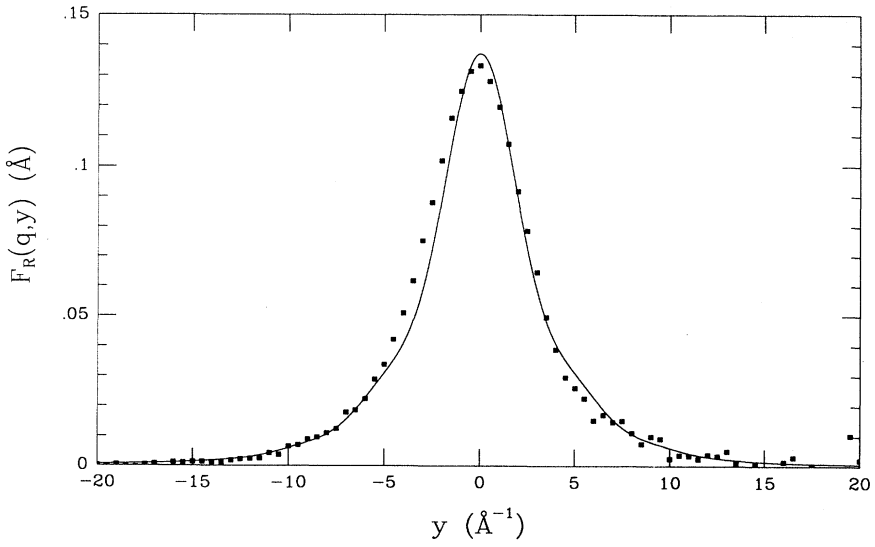

FIG. 6. Experimental data (dots) and theoretical scaling function, $F_R(q,y)$ [Eq. (22)] (solid line) for H_2. Experimental data and resolution function used in Eq. (22) are from Ref. 9, Fig. 1(c). Parameters used are $E_k=70$ K, $M=1$ a.m.u., $r_0=0.74$ Å, and $\sigma_T=1.4$ Å^{-1}. The resolution function is described by a Lorentzian of width 0.67 Å^{-1}.

transfer region ($q \approx 100$ Å^{-1}; experimental data correspond to Fig. 1(c) of Ref. 9). From Fig. 5 it can be seen that the convolution of the vibrational motion with the translation motion, via Eq. (14), still produces a significant decrease in intensity of the recoil peak and smears out the oscillation centered around 5 Å^{-1}. Therefore the translational motion, as already observed in the case of D_2, is important in that determines a quantitative change of the overall shape of the scaling function. In previous model calculation results on H_2, the interaction process is described as the scattering of a neutron off a proton which has a vibrational kinetic energy equal to one-half of the total vibrational kinetic energy and a value for r_0 equal to one half the actual value for the H_2 molecule. As a consequence the whole shape of the scaling function of Ref. 9 for the vibrational motion is different from the result of our approach (e.g., the oscillatory behavior of the scaling function of Ref. 9 occurs around 8 Å^{-1}, see Fig. 3 of Ref. 9). The effect of the convolution needed to obtain $F_R(q,y)$ with, first the center-of-mass motion and, second, with the experimental resolution function, largely washes out the differences in the shape of the vibrational scaling functions. From Fig. 6 is clear that a good agreement between our calculation and the experimental data is obtained. The minor shift towards $y<0$ present in the data is to be ascribed to the finite q values of the experiment. We stress that our calculation does not make any use of free parameters.

V. CONCLUSIONS

In this paper a proper theoretical framework has been presented for the calculation of momentum distributions of nuclei within diatomic molecules and for obtaining the asymptotic scaling function for neutron scattering at very high-momentum transfer for both homonuclear and heteronuclear molecules. From Figs. 4 and 6 one concludes that the results of our approach provide a description of the experimental asymptotic scaling function in both D_2 and H_2, without any fitting procedure involved.

From the results presented above one can conclude that for a stringent test of the dynamics of a single nucleus in diatomic liquids or solids two demands are essential. A first one is to work with the best and accurately known experimental resolution function and a second one is to work at the highest possible q values, which would provide experimental data more safely described within the IA, and hence allow a good check of the reliability of the present calculation. In DINS experiments both the above requirements can be accomplished; for example, in the case of D_2 one could be able to decrease the influence of the instrumental resolution performing the experiment in a higher momentum transfer region, i.e., in the scattering range $90° < 2\theta < 180°$.

As a final comment, it is well known that less severe resolution contributions are available in experiments performed on direct geometry spectrometer (DGS), where the energy selection is done on the incident neutron flux. In this case, due to the lower ω and q values accessible as compared to eVS spectrometer, the transition region from the scattering off the molecule and the scattering off the single nuclei in the molecule can be explored.[5] This kind of experiment's results can be extremely important also for a precise determination of the translational kinetic energy, whose knowledge is essential to perform a quantitative comparison of theoretical and experimental asymptotic scaling functions.

ACKNOWLEDGMENTS

The authors wish to thank Dr. D. Colognesi, Professor M. Nardone, and Dr. J. Mayers for many stimulating discussions and suggestions. A special thank you goes to Dr. J. Mayers also for having provided us with the experimental data on D_2 and H_2.

[1] A. C. Evans, J. Mayers, D. N. Timms, and M. J. Cooper, Z. Naturforsch. Teil A **48** 425 (1993).
[2] S. W. Lovesey, *Theory of Neutron Scattering from Condensed Matter* (Oxford University Press, London, 1987), Vol. 1; P. C. Hohenberg and P. M. Platzmann, Phys. Rev. **152**, 198 (1966).
[3] B. Williams, *Compton Scattering* (McGraw-Hill, New York, 1977).
[4] C. Ciofi degli Atti, E. Pace, and G. Salmé, Phys. Rev. C **43**, 1155 (1991).
[5] W. Langel, D. L. Price, R. O. Simmons, and P. E. Sokol, Phys. Rev. B **38**, 11 275 (1988).
[6] K. W. Herwig, J. L. Gavilano, M. C. Schmidt, and R. O. Simmons, Phys. Rev. B **41**, 96 (1990).
[7] K. W. Herwig, P. E. Sokol, T. R. Sosnick, W. M. Snow, and R. C. Blasdell, Phys. Rev. B **41**, 103 (1990).
[8] C. Andreani, A. Filabozzi, M. Nardone, F. P. Ricci, and J. Mayers, Phys. Rev. B **50**, 12 744 (1994).
[9] J. Mayers, Phys. Rev. Lett. **71**, 1553 (1993).
[10] G. B. West, Phys. Rep. **18**, 263 (1975).
[11] J. Van Kranendonk, *Solid Hydrogen* (Plenum, New York, 1983).
[12] *Comprehensive Inorganic Chemistry*, edited by A. F. Trotman-Dickenson (Pergamon, New York, 1973), Vol. 1.
[13] C. Andreani, G. Baciocco, R. S. Holt, and J. Mayers, Nucl. Instrum. Methods A **276**, 297 (1989).
[14] J. Mayers and A. C. Evans (unpublished).
[15] C. Andreani, V. Merlo, and M. A. Ricci, Nucl. Instrum. Methods B **36**, 216 (1989).
[16] C. Andreani, V. Merlo, E. Pace, and P. Postorino, Phys. Lett. A **171**, 76 (1992).